Earth and Space Science

RESEARCH ARTICLE
10.1029/2021EA001825

Reactivation Potential of Intraplate Faults in the Western Quebec Seismic Zone, Eastern Canada

Jeremy M. Rimando[1] **and Alexander L. Peace**[1]

[1]School of Earth, Environment & Society, McMaster University, Hamilton, ON, Canada

Key Points:

- NW-SE-striking faults in the western Quebec seismic zone are more likely to be reactivated under the present-day tectonic stress field
- Slip tendency analysis is applicable to identifying potentially active faults in stable continental regions

Supporting Information:

Supporting Information may be found in the online version of this article.

Correspondence to:

J. M. Rimando,
rimandoj@mcmaster.ca

Citation:

Rimando, J. M., & Peace, A. L. (2021). Reactivation potential of intraplate faults in the western Quebec seismic zone, eastern Canada. *Earth and Space Science*, *8*, e2021EA001825. https://doi.org/10.1029/2021EA001825

Received 28 APR 2021
Accepted 1 JUL 2021

Abstract The intraplate western Quebec seismic zone (WQSZ) in eastern Canada experiences moderate seismicity that mainly results from reactivation of inherited structures under the present-day, NE-SW-striking regional maximum horizontal stress (S_H) and, possibly to a minor extent, through stress perturbations in response to glacio-isostatic adjustment. This work comprises the first numerical stress simulation-based study that predicts the preferred spatial distribution, trends, and sense of slip of contemporary fault reactivation, which may have implications for possible fault segmentation patterns in the WQSZ. We show that mostly NNW-SSE to NW-SE-striking faults exhibit the highest slip tendency values. Spatial patterns of slip tendency and kinematics of reactivation are consistent with the observed seismicity. In an area where Quaternary-active faults have yet to be systematically identified, we have narrowed down areas to focus on for more detailed, future neotectonic investigations that could provide sound foundation for seismic hazard assessments. This study demonstrates the applicability of slip tendency analysis to identifying potentially active faults in stable continental regions worldwide.

1. Introduction

The western Quebec seismic zone (WQSZ; Figure 1) in eastern Canada is an intraplate continental region characterized by spatial clustering of weak to moderate recent seismicity (Figure 2). This seismicity likely results mainly from the reactivation under the present-day tectonic stress field of inherited structures such as late Precambrian to early Paleozoic Iapetan rifts and aulacogens, as well as Precambrian suture zones and plate boundaries (Culotta et al., 1990; Kumarapeli, 1978; Rimando, 1994; Rimando & Benn, 2005). Major tectonic features in the area include grabens and half-grabens that belong to the Saint Lawrence Rift system, such as the Ottawa-Bonnechere and Timiskaming grabens (Figure 1a), that are composed primarily of NW-SE- and NE-SW-striking, steeply dipping valley-forming faults (Figures 1a and 1b; Kay, 1942; Lamontagne et al., 2020, and references therein; Lovell & Caine, 1970). These affect the Precambrian basement of the Canadian Shield and the Paleozoic sedimentary sequences of the Saint Lawrence-Ottawa Platform, and are associated with most of the topographic relief in this region (Figure 1). The current tectonic stress field in eastern North America is well constrained and, as with most other continental plate interiors, is broadly uniform (Mazzotti & Townend, 2010). Borehole breakout measurements and inversions of earthquake focal mechanisms consistently indicate a maximum horizontal compressive stress axis (S_H) that is oriented NE-SW (Mazzotti & Townend, 2010; Reiter et al., 2014; Snee & Zoback, 2020), which is attributed to spreading along the Mid-Atlantic Ridge (Richardson, 1992).

Remarkably, despite the seismicity, only a handful of active faults with surface expression in the WQSZ have been identified and mapped to date. In the WQSZ, the Timiskaming Graben (Figure 1b), for instance, has been identified as active from seismotectonic analysis and from the evidence of coseismic ground deformation following the 1935 moment magnitude (M_W) 6.1 Timiskaming earthquake (Figures 2a and 2b; Bent, 1996; Doughty et al., 2012). The location, NW-SE strike, and reverse faulting kinematics determined from detailed analysis of the source mechanism for this earthquake by Bent (1996) are consistent with fault reactivation along the NW-SE-striking Timiskaming graben. Conversely, some recent earthquakes, such as the 2010 M_W 5.2 Val des Bois (Atkinson & Assatourians, 2010; Ma & Motazedian, 2012) and 2013 M_W 4.7 Ladysmith earthquakes (Ma & Audet, 2014), are associated with well-defined source mechanisms and locations, but have yet to be associated with their causative faults. Eastern Canada, including the WQSZ, is currently lacking a comprehensive, reliable assessment of seismic hazards, due to the scarcity of detailed earthquake source models, typically from a combination of seismic, geologic, and/or geodetic data (Morell et al., 2020). Further complicating the poor understanding of fault reactivation and seismicity in eastern

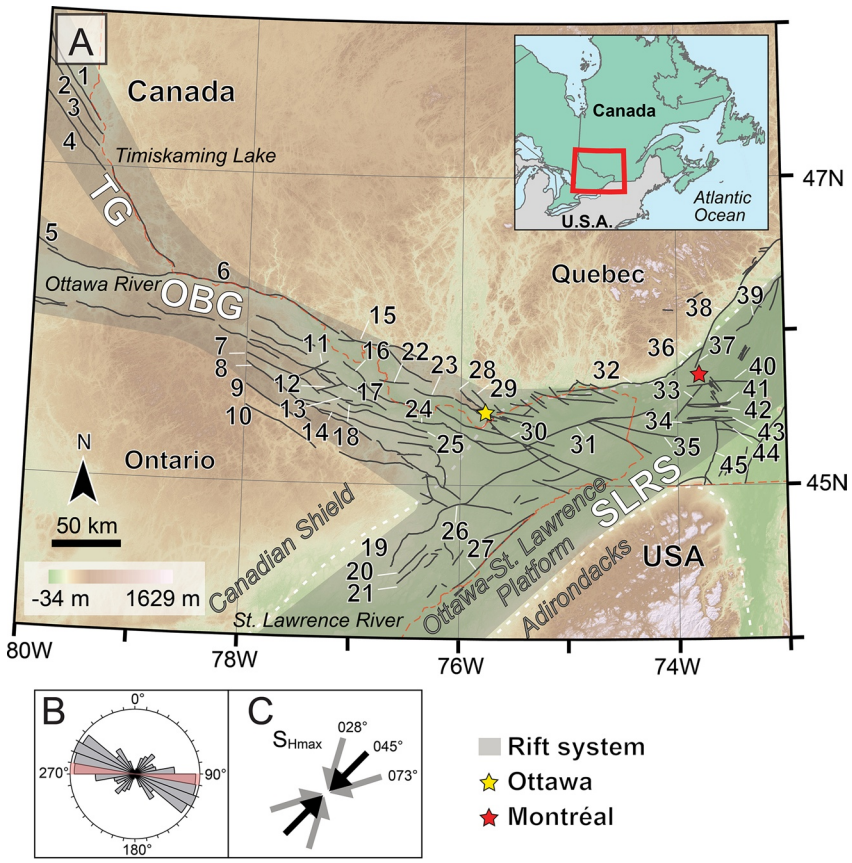

Figure 1. (a) Major tectonic features and faults of the western Quebec seismic zone (WQSZ). TG—Timiskaming Graben. OBG—Ottawa-Bonnechere Graben. SLRS—Saint Lawrence Rift System. White dashed line indicates the boundaries of geological provinces: Canadian Shield, Ottawa-St. Lawrence Platform, and the Adirondacks. Red dashed line indicates political boundaries. Inset map shows the location of the WQSZ in eastern North America. Faults with names are labeled as follows: 1—Timiskaming, 2—Cross Lake, 3—Montréal River, 4—Latchford, 5—Crystal Falls, 6—Mattawa River, 7—Deacon, 8—St. Patrick, 9—Hopefield, 10—Madawska, 11—Gardez Pieds, 12—Cochran, 13—Eganville, 14—Shamrock, 15—Coulonge, 16—Muskrat, 17—Dore, 18—Douglas, 19—Canoe-Dessert Lake, 20—Sydenham Lake, 21—Loughborough Lake, 22—Rocher Fendu, 23—Eardley, 24—Hazeldean, 25—Packenham, 26—Rideau Lakes, 27—St. Lawrence River, 28—Meech Lake, 29—Gatineau River, 30—Gloucester, 31—Russel Rigaud, 32—Lachute, 33—Milles Iles, 34—Sainte-Anne-de-Bellevue, 35—Sainte-Justine, 36—New-Glasgow, 37—Sainte-Julienne, 38—Saint-Maurice, 39—Saint-Cuthbert, 40—Bas-de-Sainte-Rose, 41—Rapide-du-Cheval Blanc, 42—Ile Bizard, 43—Dorval, 44—Saint-Regis, 45—Havelock. The topography is derived from a 30-m-resolution Advanced Spaceborne Thermal Emission and Reflection Radiometer global digital elevation models (https://asterweb.jpl.nasa.gov/gdem.asp) and the fault traces are from the Geological Survey of Canada's WQSZ faults map (Lamontagne et al., 2020). (b) The orientations of the 210 WQSZ faults are summarized in a rose diagram which has 18 bins (10° intervals). (c) S_{Hmax} orientations in the WQSZ (Mazzotti & Townend, 2010); 045° is the average regional stress orientation, while 028° and 073° are the extreme values.

Canada is the fact that most evidence of initiation of fault activity under the current stress regime typically postdates glaciation (Adams, 1989). There has been a debate over whether recent faulting occurs as a result of tectonic stress or glacio-isostatic adjustment, or both (e.g., Adams, 1989; Brooks & Adams, 2020; Wallach et al., 1995). Despite the surficial nature and exposure of some pop-up structures and offset boreholes within quarries in Ontario and Quebec, a tectonic origin is a preferred interpretation for most of these features due to the compatibility of their orientations and kinematics with the current regional stress field in eastern North America (Wallach & Chagnon, 1990; Wallach et al., 1993, 1995). Besides, detailed studies of the state of stress in eastern Canada (Mazzotti & Townend, 2010) indicate that magnitudes of long-wavelength stress perturbations such as postglacial rebound stresses are an order of magnitude lower, hence minor in comparison to mid-crustal stresses. It is possible, however, for postglacial rebound stress to cause high enough stress perturbations if these are concentrated on faults with an unusually low coefficient of friction ($\mu \sim 0.1$)

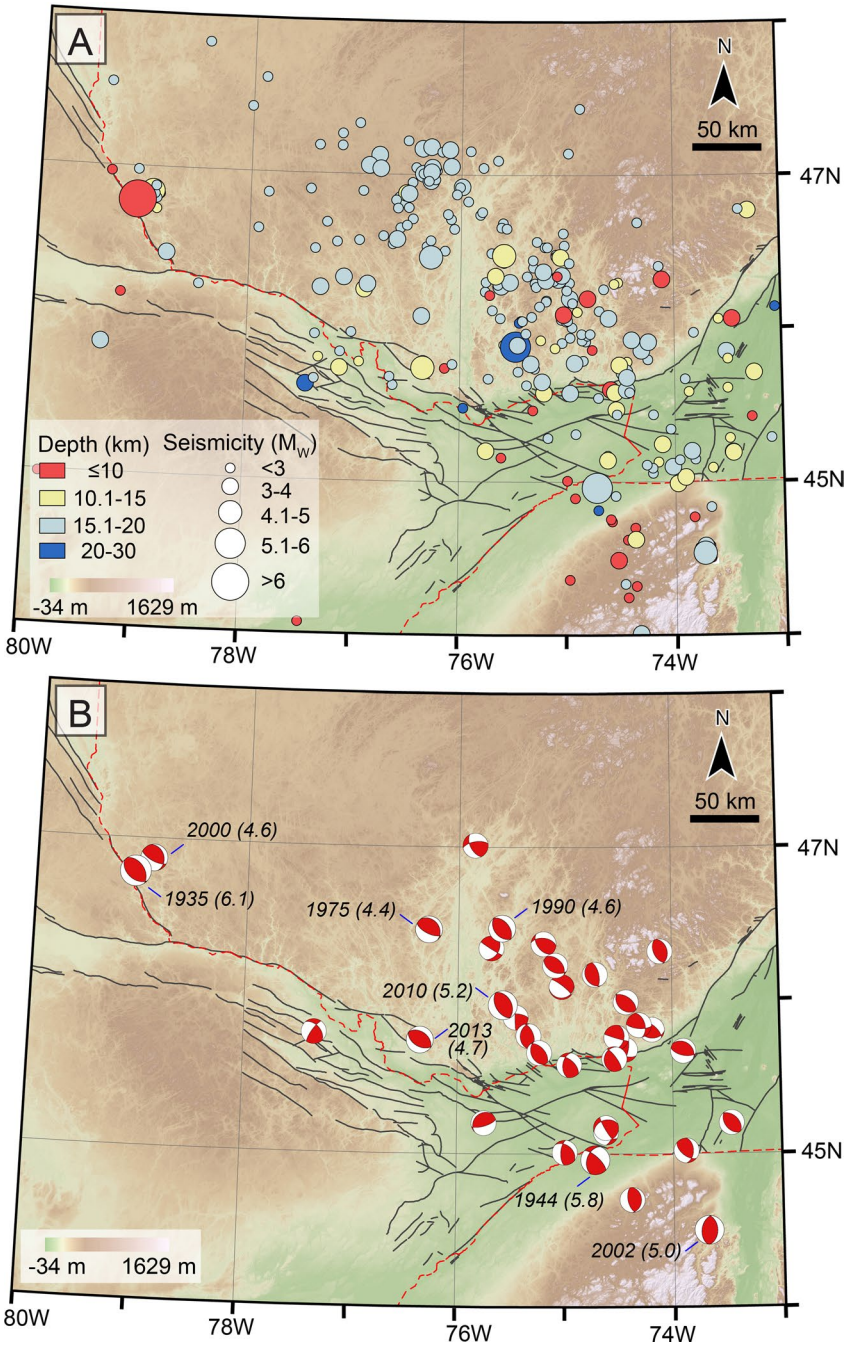

Figure 2. Seismicity in the western Quebec seismic zone (WQSZ). (a) Earthquake epicentral plots are color-coded according to depth and scaled to magnitude. (b) Earthquake focal mechanisms with labels of year and magnitude of notable events. Well-localized seismicity is from Adams et al. (1988, 1989), Bent (1996), Bent et al. (2002, 2003), Du et al. (2003), Horner et al. (1978), Ma and Eaton (2007), Seeber et al. (2002), Wahlström (1987), and the earthquake bulletins of both the Natural Resources Canada (https://earthquakescanada.nrcan.gc.ca/index-en.php) and the United States Geological Survey (https://www.usgs.gov/natural-hazards/earthquake-hazards/earthquakes).

(Mazzotti & Townend, 2010). An alternative theory for the enhanced seismicity in the WQSZ, which forms an NW-SE-striking linear cluster of intermediate focal depth (8–18 km) earthquakes across eastern Canada, is the passage of North America over the Great Meteor Hotspot in the Mesozoic. This theory postulates that thermo-mechanical weakening of ancient faults and shear zones was caused by the Great Meteor Hotspot along the interpreted NW-SE-trending hotspot track (e.g., Dineva et al., 2007; Ma & Eaton, 2007, and

references therein), and that present-day seismicity are unusually long-lived aftershock sequences of large past earthquakes (e.g., Stein & Liu, 2009). Shallow seismicity (<8 km), however, appears to be more randomly distributed throughout the region and cannot be accounted for by this theory. In addition, it is not clear why seismicity would be sustained to the present-day through this thermal weakening mechanism.

Knowledge of the nature, distribution, and extent of seismogenic structures in Eastern Canada, including their potential for causing large magnitude earthquakes, is of paramount socio-economic importance (e.g., Morell et al., 2020). A major earthquake in eastern Canada could trigger a chain of events in the insurance industry and have far-reaching economic consequences (Le Pan, 2016). However, there is currently no map of the active structures in the WQSZ, a region that hosts major population centers, including Ottawa and Montréal. As in most intraplate settings, there is a rarity of well-preserved recent fault/fold scarps in the WQSZ (McCalpin, 2009), probably as a result of long recurrence intervals on slow-moving faults (Stein, 2007), and due to glacial peneplanation (Dyke et al., 2002). Similarly, the short temporal coverage of instrumental seismicity records is not enough to create an inventory of detailed earthquake source models and to determine earthquake recurrence intervals in intraplate regions. However, we know from global examples that large earthquakes are far more common than previously thought in "stable continental regions" (Calais et al., 2016; Rimando et al., 2021). In eastern North America, instrumental, historical, and paleoseismic records show that the region has been shaken by devastating earthquakes, such as the 1929 M_S 7.2 Grand Banks and the 1811–1812 M_W 7.2–8.2 New Madrid earthquakes (Bent, 1995; Hasegawa & Kanamori, 1987; Tuttle et al., 2002). There is a wealth of studies on the occurrence of paleoearthquakes in the WQSZ, inferred from subaqueous mass transport deposits and liquefaction features. However, these have yet to be linked with specific earthquake-generating faults (Aylsworth & Hunter, 2003; Brooks, 2013, 2014, 2015; Brooks & Adams, 2020).

Ottawa is the seat of Canada's national government and Montréal has the second-largest economy (based on GDP) in Canada (Statistics Canada, 2020a). Both are major national and global commercial, financial, technological, and cultural hubs. As of 2020, the total population in the Ottawa-Gatineau and Montréal metropolitan areas is over 5.5 million (Statistics Canada, 2020b). Despite the economic and political importance of these areas, infrastructure in these cities is mostly old and is likely to be ill-prepared for possible future strong ground shaking during an earthquake (Goda, 2019; Kovacs, 2010; Mirza & Ali, 2017). Mapping of active faults is therefore critical to estimating the seismic hazard in an area and, consequently, to formulating a reliable building code.

In the absence of a map of active faults, a good first step is to determine the potential of pre-existing faults to be reactivated under the current stress field. A good correlation between relatively high slip tendency and evidence of Quaternary activity has been shown in different tectonic settings with wide-ranging levels of seismic activity (e.g., Worum et al., 2004; Yukutake et al., 2015). For instance, in Japan, most faults that exhibited relatively high slip tendency values (slip tendencies of ≥ 0.6) were consistent with faults that were classified independently as active (Yukutake et al., 2015). While previous studies have described the likely orientation and kinematics of fault reactivation conceptually under the current stress field (Daneshfar & Benn, 2002; Rimando, 1994; Rimando & Benn, 2005), no work has characterized in detail the slip tendency and expected slip kinematics of specific faults in the WQSZ. This work presents the first study which uses 3D numerical stress simulations to explore the preferred spatial distribution and trends, and predicted sense of slip of reactivated pre-existing structures in the WQSZ under the current tectonic stress field. We show how fault reactivation potential studies can be useful for identifying key areas or fault populations to focus on for more detailed seismic hazard assessment.

2. Data and Methods

Slip tendency (Morris et al., 1996) is the ratio of the shear stress to the normal stress on a fault surface, which is expressed as the following equation:

$$T_s = \tau/\sigma_n, \tag{1}$$

where T_S is the slip tendency, τ is the shear stress, and σ_n is the normal stress.

Slip tendency analysis has been used in different tectonic settings worldwide to characterize the relative likelihood of populations of faults to slip under current or past stress fields (e.g., Morris et al., 1996; Peace et al., 2018; Worum et al., 2004). Faults that are likely to slip are those with a higher ratio of shear stress to normal stress. Faults subject to a certain stress field are characterized as "optimally oriented" if the set of strikes and dips yield high slip tendency values.

It should be noted, however, that we make implicit assumptions in using this technique, which introduce some limitations on how closely our model represents reality. Following the Wallace (1951) and Bott (1959) hypothesis wherein slip on faults is expected to occur along the direction of the maximum resolved shear stress, this method assumes simple planar faults and a relatively uniform stress field, and it neglects fault interaction, fault block rotation, and internal deformation. Despite these caveats, it has been shown through numerical studies to be a good first-order approximation (Dupin et al., 1993; Pollard et al., 1993), as the deviation between actual and theoretical slip kinematics are on average less than 10°. A strong match between modeled slip tendencies and directions and natural reactivated fault plane orientations and slip kinematics from global geological and seismological data sets lends support to the use of slip tendency analysis as a useful prediction tool (Collettini & Trippetta, 2007; Lisle & Srivastava, 2004).

We modeled the reactivation potential of faults in the WQSZ using the "Slip Tendency" function in the "Stress Analysis" module of the software Move™ by Petroleum Experts Limited (https://www.petex.com/), and determined the predicted sense of fault slip using the "Slicken 1.0" software (Xu et al., 2017). In both software packages, the stress tensor and fault plane orientations were the required inputs.

We primarily used the average regional stress orientation of 045° but also ran simulations using the extreme values (028° and 073°) determined for the Montréal and Gatineau zones by Mazzotti and Townend (2010). These were based on Bayesian inversion of earthquake focal mechanisms and calculation of the weighted averages (weights based on quality) of borehole breakout stress measurements within 250 km of the area of interest. The orientations of S_H measured from both sources were consistent and roughly parallel. Focal mechanism inversions revealed a nearly vertical σ_3 and nearly horizontal σ_1 and σ_2, defining a reverse faulting stress regime, which is consistent with findings of previous crustal stress orientation studies (Heidbach et al., 2010; Reiter et al., 2014; Snee & Zoback, 2020). Knowing that σ_1 is horizontal enabled us to use the S_H from borehole measurements as an approximation for σ_1.

We estimated regional stress magnitudes by assuming a critically stressed crust (Townend & Zoback, 2000; M. D. Zoback & Zoback, 2002), in which differential stress values are at a level such that optimally oriented Andersonian faults are on the verge of slipping. In a reverse-faulting stress regime, the principal stresses can be computed using the following equations:

$$\sigma_1 - \sigma_3 = \rho g z\left(\lambda - 1\right)\left(1 - F\right), \tag{2}$$

$$\sigma_3 = \left(1 - \lambda\right)\rho g z, \tag{3}$$

$$R = \frac{\sigma_1 - \sigma_2}{\sigma_1 - \sigma_3}, \tag{4}$$

$$F = \left(\sqrt{\mu^2 + 1} + \mu\right)^2, \tag{5}$$

where σ_1 is the maximum horizontal stress, σ_2 is the minimum horizontal stress, σ_3 is the vertical stress, λ is the pore-fluid factor (pore fluid pressure, P_f divided by the σ_3), ρ is the average crustal density (2,700 g/m^3), g is the gravitational acceleration (9.8 m/s^2), z is the depth (in m), R is the principal stress difference ratio (typically 0.6 in this intraplate continental region), F is the frictional parameter, and μ is the coefficient of friction.

We calculated the stress magnitudes at a mid-seismogenic zone depth of 10 km. Our choice of coefficient of friction (μ) and pore fluid factor (λ) values considers the fact that the maximum possible differential stress

(σ_1−σ_3) values at mid-crustal depths in this region are unlikely to exceed 200 megapascals (MPa), which is based on previous modeling studies and extrapolation of in situ field measurements at shallower depths in Canada and in intraplate settings in general (e.g., Hasegawa et al., 1985; Lamontagne & Ranalli, 1996, and references therein). This condition of relatively low differential stress necessitates the μ and λ values to be lower and higher, respectively, than the values that are commonly assumed (e.g., Byerlee, 1978; Townend & Zoback, 2000). For the purposes of this study, we used a σ_1−σ_3 value close to the 200 MPa upper limit. We adapted a μ of 0.5 and a λ of 0.6, which are intermediate to the values previously determined from modeling of the conditions for slip of earthquakes in southeastern Canada (M. L. Zoback, 1992). A low coefficient of friction at shallow depths likely results from the presence of thick phyllosilicate-rich fault gouges (e.g., den Hartog et al., 2020) and in the mid-crust through the presence of a dense network of fractures and faults (Ito & Zoback, 2000). The upward migration of mantle-derived mixed H_2O-CO_2 fluids is a proposed source of high pore fluid pressure that enables the reactivation of high-angle faults in eastern Canada (Sibson, 1989). Hence, we applied the following stress tensors in our analyses: σ_1 = 028°–073° = 277.09 MPa, σ_2 = 118°–163° = 174.34 MPa, and σ_3 = vertical = 105.84 MPa (Figure 1c; Mazzotti & Townend, 2010).

With the exception of a few faults (e.g., Doughty et al., 2012), information on the deeper structure of most faults is lacking in the WQSZ. Where available, information on the geometry of faults from subsurface imaging techniques is confined to depths of less than 100 m at best (e.g., Doughty et al., 2012). However, most papers, reports, and geological cross-sections on the area indicate steep fault dips with an average of around 60° (e.g., Lovell & Caine, 1970; Rimando, 1994; Rocher & Tremblay, 2001). We therefore assumed a dip of 60° to build 3D fault surface models. The 3D models were built by projecting surfaces from shapefiles of the Geological Survey of Canada's latest WQSZ faults map (Lamontagne et al., 2020). We also ran simulations over a range of fault dips (at 15° increments) to test the effect of underestimating or overestimating the actual fault dip on the calculated slip potential and sense of slip of faults.

3. Results

Our slip tendency analysis reveals that under the present-day regional stress field (Figure 1c), and assuming a dip of 60° on faults in the WQSZ, mostly NNW-SSE to NW-SE striking faults tend to have relatively higher slip tendencies (compared to the more NE-SW-striking faults in the eastern sector), and are therefore, considered optimally oriented to be reactivated (Figure 3a). Faults are predicted to slip mostly either as pure reverse faults or as oblique reverse faults (Figure 3b). The magnitude and spatial distribution of the slip tendency varies, albeit insignificantly, over the range of the assumed possible orientations of σ_1 (i.e., 028°, 045°, and 073°). For instance, the average slip tendency values of NW-SE-striking and NE-SW-striking faults (for 60° dip) vary on average by ~5% and ~10% of each other, respectively (Figure 3a and Table S1). On the other hand, the preferred kinematics of slip has a more noticeable spatial variation. Faults that are oriented perpendicularly to σ_1 are expected to be reactivated with a pure reverse slip. Consequently, the distribution of pure reverse faults appears to rotate clockwise as the σ_1 azimuth is rotated clockwise, and coincidentally, decreases in abundance due to the decreasing number of faults oriented at a high angle to the σ_1 in the WQSZ (Figure 3b). While the magnitudes of slip tendency appear to vary as a function of the assumed fault dip, the NW-SE striking faults of the WQSZ mainly exhibits generally relatively higher slip tendencies, with average values being 20% higher than NE-SW-striking faults for σ_1 = 045° (Figure 4; Table S1). The predicted slip in the 15°–60° dip scenarios all exhibit either pure reverse or oblique reverse faulting. It is notable that in the 75° dip scenario, there tends to be significantly more faults with a dominant strike-slip component, and in the 90° dip scenario, faults are expected to be reactivated almost entirely as pure strike-slip faults (Figure 5). Additionally, for faults dipping 75° and 90° with σ_1 = 028° and 045°, NE-SW-striking faults tend to have slightly higher average slip tendency values than NW-SE-striking faults, possibly due to these faults being optimally oriented to be reactivated with a dominant strike-slip component (Figures S1–S4; Table S1). It is worth noting that, with the exception of the 30° dip scenario (which seems to be the near-optimal dip for fault reactivation in the WQSZ), slip tendency values decrease as the assumed fault dip increases (Figure 4). Most of these observations on the variations of slip tendency and expected slip kinematics as a function of dip and as a function of σ_1 orientation, apply as well to other σ_1 orientation scenarios (σ_1 = 028° and σ_1 = 073°) and to the different dip scenarios (15°, 30°, 45°, 75°, and 90°), respectively (Figures S1–S4).

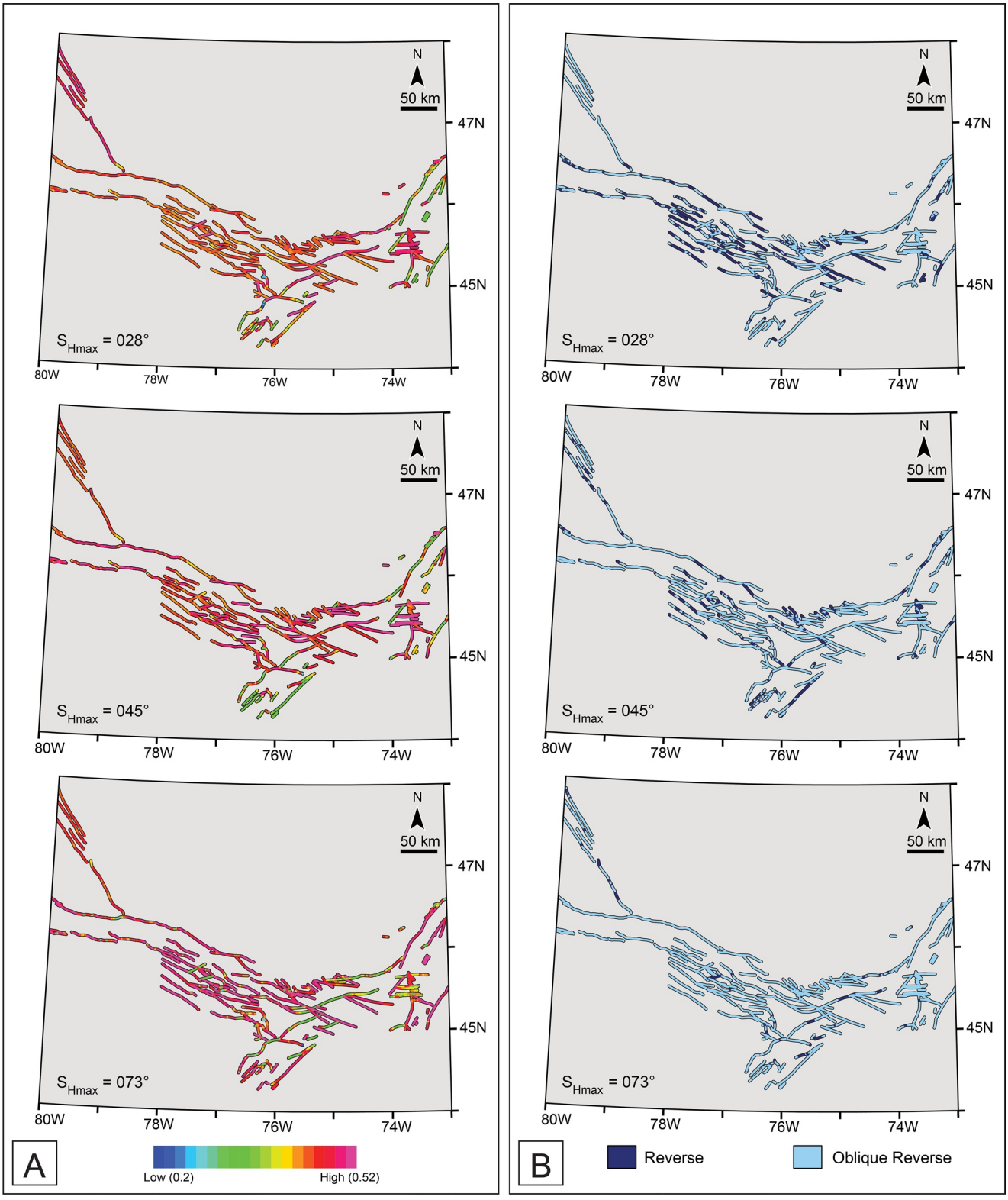

Figure 3. (a) Slip tendency maps and (b) predicted slip kinematics of faults dipping 60° with S_H azimuth values of 028°, 045°, and 073°.

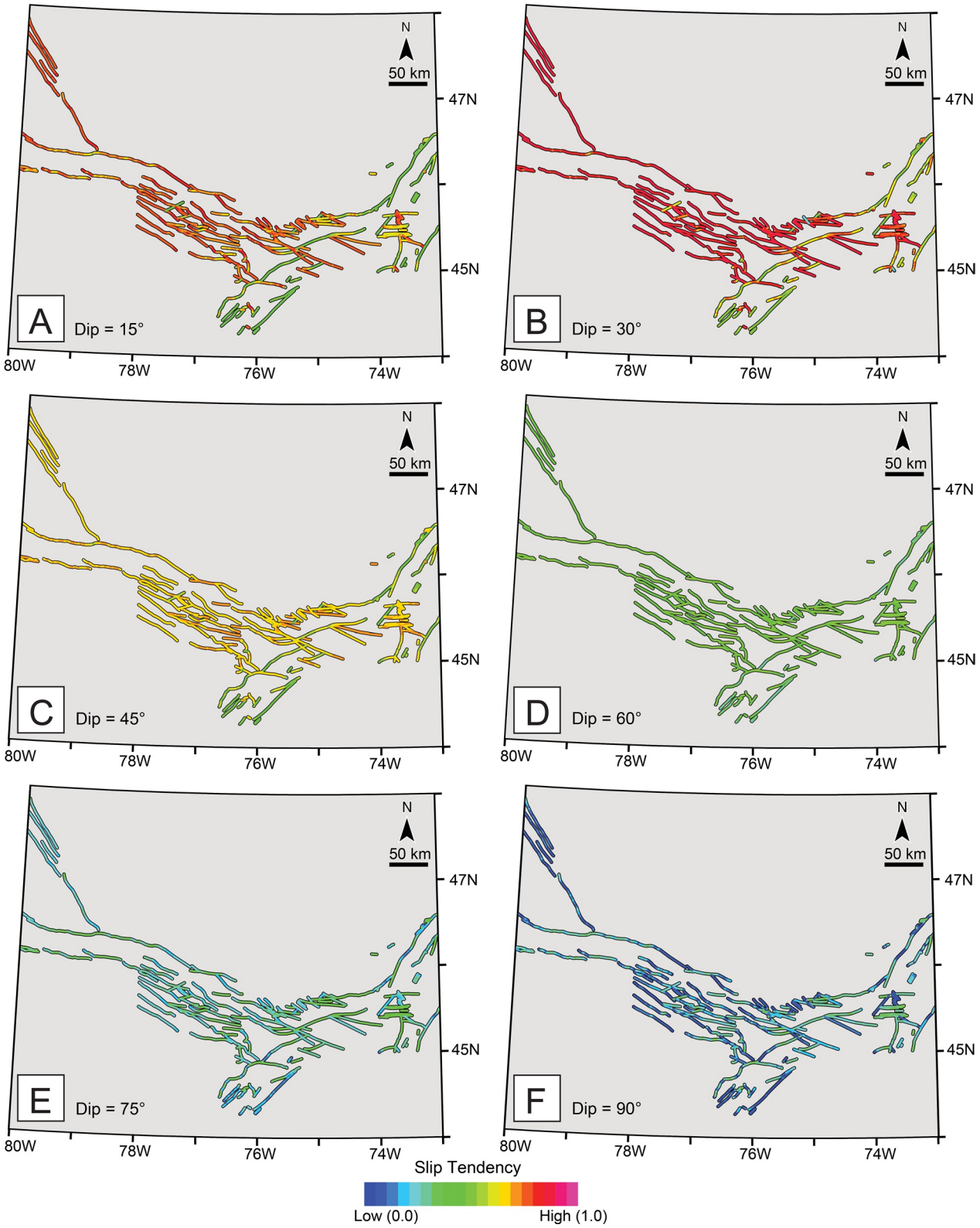

Figure 4. Slip tendency maps for different fault dip scenarios (with an S_H azimuth of 45°). (a) 15°, (b) 30°, (c) 45°, (d) 60°, (e) 75°, and (f) 90°.

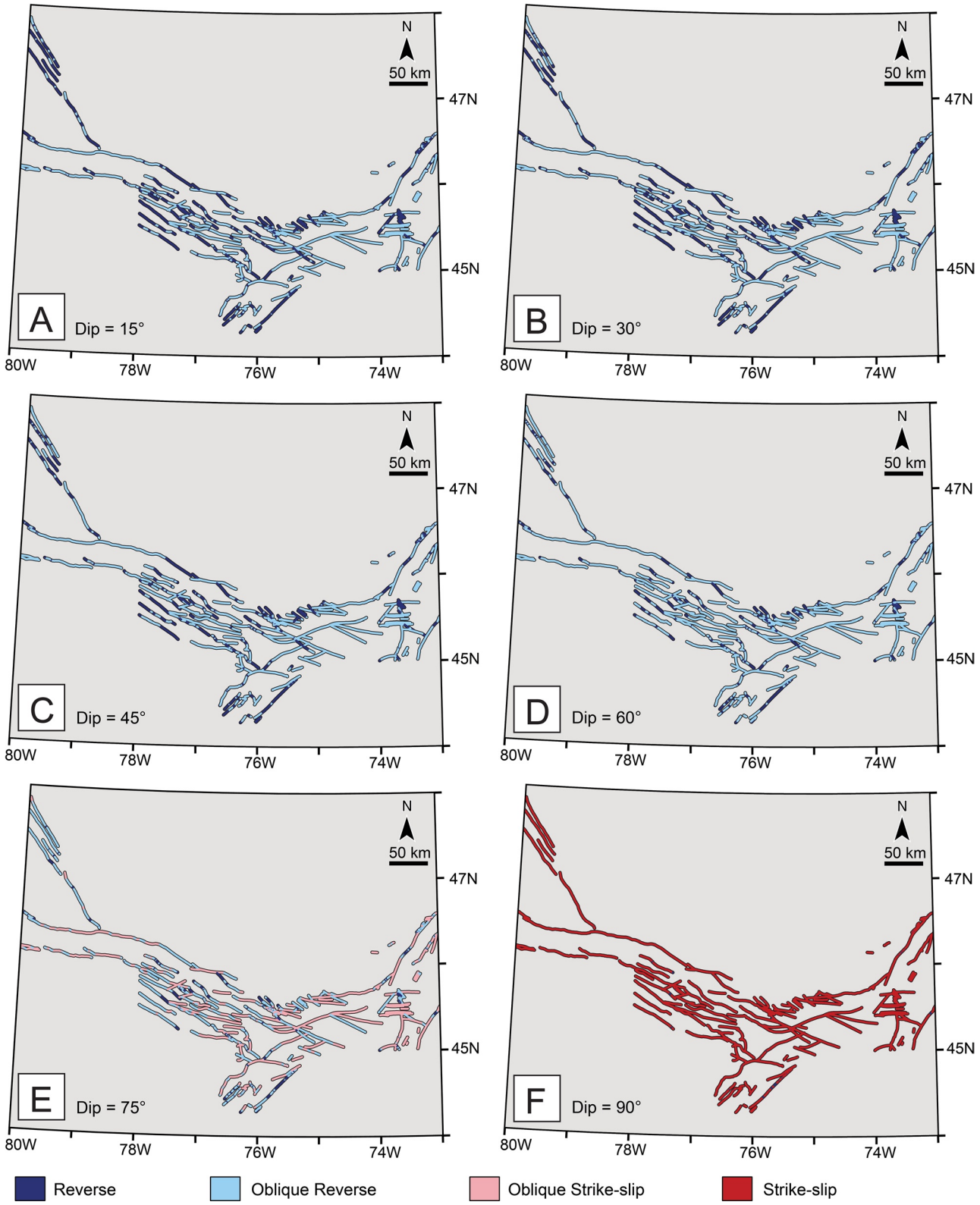

Figure 5. Predicted slip kinematics for different fault dip scenarios (with an S_H azimuth of 45°). (a) 15°, (b) 30°, (c) 45°, (d) 60°, (e) 75°, and (f) 90°.

4. Discussion and Conclusions

Our results show that the NNW-SSE-striking to NW-SE-striking faults of the WQSZ consistently exhibit relatively higher slip tendency values. However, although we considered the effect of adapting different dip values, we modeled dips uniformly across the WQSZ during each simulation. In reality, however, it is unlikely the case that the dips of all the faults in the WQSZ are uniform. Nonetheless, unless the faults in the west sector are all dipping vertically or nearly vertically, and assuming that the Wallace (1951) and Bott (1959) hypothesis applies and pore fluid pressure conditions and fault frictional properties vary insignificantly throughout the WQSZ, then the slip tendency values of the NW-SE-striking faults, mostly to the west of the WQSZ, are expected to be higher for most conceivable variable-dip scenarios.

There is also a good correspondence between the modeled kinematics of fault reactivation (i.e., predominantly reverse and oblique reverse) (Figures 3b and 5) under the assumed range of stress tensors and the actual kinematics of recent natural seismicity as indicated by earthquake focal mechanisms (Figure 2b). Additionally, in upstate New York and southeastern Ontario, previous work has demonstrated that recent natural seismicity is spatially associated dominantly with the NW-SE-striking population of faults (Daneshfar & Benn, 2002; Rimando, 1994). Therefore, there seems to be multiple lines of evidence that give credence to the results of our modeling.

In reality, however, the assumptions of Wallace (1951) and Bott (1959) are rarely entirely met (Lisle, 2013), which could feasibly cause deviations between our modeling results and the actual fault activity and kinematics. The results of this study, nonetheless, should provide a first-order approximation of the distribution of fault activity in the WQSZ. It can be argued, however, that the orientation of stress is fairly homogenous in the region, and the effects of fault block rotations and fault interactions are unlikely to significantly affect our results given the scale of our study area and the resolution of our modeling. After all, it is possible that the objections to the assumptions of the Wallace-Bott hypothesis may apply only at a relatively local scale (Lisle, 2013).

Future numerical stress simulations would benefit from more detailed 3D fault geometry models. For instance, some faults in the region have been shown to exhibit flat-ramp-flat and listric fault geometries (Busch et al., 1996; Rimando & Benn, 2005), which could possibly result in more complex along-strike and down-dip patterns of slip tendency and slip kinematics. Future studies should consider improving 3D fault models by integrating data from geophysical subsurface imaging, natural and trenching exposures, and seismicity. Having such data will not only reduce the uncertainty in our modeling, but will also help address concerns regarding the validity of the approach used in this study.

While fault slip in the WQSZ could very well be mainly tectonic in nature, glacial unloading could play an important role as a trigger (Wu & Hasegawa, 1996). In reverse/thrust faulting stress regimes such as in the WQSZ (M. L. Zoback, 1992), glacial unloading could possibly decrease the magnitude of the vertical σ_3, resulting in a higher differential stress (e.g., Muir-Wood, 1989). The extent to which glacio-isostatic adjustment can influence the regional stress field and, consequently, the modeled distribution of slip tendency of faults in the WQSZ should also be further explored in future work. Ongoing isostatic rebound in eastern Canada (George et al., 2012) can be modeled by progressively increasing the differential stress.

Our findings on the range of conditions in which faults in the WQSZ may experience reactivation have implications for the assessment of seismic hazards in the area. For instance, possible fault segmentation can be inferred from our slip tendency and slip kinematics maps (e.g., Figure 3). In the absence of documented actual earthquake rupture segments, which is the case in the WQSZ, structural, geologic, and geometric characteristics such as bends, stepovers, gaps, branching, intersections, and changes in the orientation and sense of slip of faults are typically used as preliminary criteria for assessing fault segmentation (e.g., DePolo, 1989; DePolo et al., 1991; Knuepfer, 1989; Rimando & Knuepfer, 2006). Assuming that the surface geometries of faults resemble the geometries at depth, the length of inferred segments can be utilized to compute possible earthquake magnitudes from empirical relationships between moment magnitude (M_W) and fault length by Wells and Coppersmith (1994). Such criteria for rupture endpoints, however, are not as clear in normal faults as they are in strike-slip and reverse faults (Knuepfer, 1989). In the WQSZ, where structures are mostly rift structures reactivated as reverse faults, interpreting segments may not be as straightforward

using these criteria since some faults may still exhibit segmentation associated with earlier periods of normal faulting.

Alternatively, examination of patterns on slip tendency and predicted slip maps, which were modeled using the present-day stress field, could allow us to identify fault segments. Endpoints of fault segments could be inferred where there are abrupt changes in slip tendency values or fault kinematics. These fault lengths can then be used to provide initial estimates of potential earthquake magnitudes from scaling relationships by Wells and Coppersmith (1994). The modeled slip type (i.e., dominantly strike-slip, reverse, or normal) could also provide further constraints for potential earthquake magnitude estimates, as calculations differ according to the type of slip (Wells & Coppersmith, 1994). Different ranges of possible earthquake magnitudes are associated with similar-length faults that have different slip-types. A 70-km-long strike-slip fault, for instance, is capable of generating M_W 7–7.4 earthquakes, while a normal fault of the same length is capable of generating a wider possible range of earthquake magnitudes of M_W 6.6–7.8 (Wells & Coppersmith, 1994). Additionally, the areal extent over which long-period ground motions occur has also been demonstrated to vary as a function of the style of faulting (Aagaard et al., 2004), and our results place constraints on the style of faulting.

While a detailed analysis of fault segmentation and estimation of the associated possible earthquake magnitudes associated with individual interpreted segments is beyond the scope of this study, we look at the example of the NNW-SSE-striking major faults that comprise the Timiskaming graben to illustrate the potential applicability of slip tendency analysis for this purpose. The Timiskaming, Cross Lake, Montréal River, and Latchford faults (faults 1–4 in Figure 1), including an unnamed fault which lies very close to the epicentral location of the 1935 M_W 6.1 Timiskaming earthquake (Figure 2), exhibit relatively high slip tendency values and slip type distributions (for $\sigma_1 = 045°$, fault dip 60°) that are fairly similar such that each fault can be considered as single segments. Assuming that the shortest mapped major fault in the OBG, the Montréal River fault (fault 3 in Figure 1), ruptures along its entire ~35-km-length, the possible associated earthquake magnitude would be at least M_W 6.6, which is much higher than the largest recorded earthquake (1935 M_W 6.1) in the vicinity. Similarly, if the other faults rupture even one-third our one-fourth of their entire length, then higher magnitudes would still be expected. More detailed mapping of late Quaternary fault traces and documentation of evidence of coseismic late Quaternary fault offsets along these optimally oriented faults, however, would be necessary to confirm the presence of such long fault segments in fact exist in the OBG.

The NW-SE-striking to WNW-ESE-striking faults starting at westernmost reach of the Ottawa-Bonnechere graben (OBG) near Crystal Falls Fault (fault 5 in Figure 1), down to the southeast at the intersection of an unnamed NW-SE-striking OBG fault with the Rideau Lakes Fault (fault 26 in Figure 1), also exhibit relatively high slip tendency values. This area is particularly promising for future neotectonic investigations as the area exhibits fault-bounded topographic relief. Detailed characterization of the tectonic geomorphology of the area could possibly reveal observable recent morphotectonic features.

The WNW-ESE-striking faults in the central OBG, from the Hazeldean Fault in Ottawa (fault 24 in Figure 1) in the west to the Ile Bizard Fault in Montréal (fault 42 in Figure 1) in the east, are also optimally oriented and, consequently, of interest for follow-up field studies. Exploring these may be more challenging, though, due to the location of faults in the center of the Ottawa River basin. Fault geometry may have to be characterized from inversions of potential field geophysical data sets (e.g., Yan et al., 2019), which have provided constraints at a variety of complex geological settings, while offset may have to be established through a combination of drilling and analysis of deep (several kilometers) seismic reflection profiles.

Finally, while this work brings us one step forward in our efforts to assess the activity of faults in the WQSZ, caution should be taken with mistaking slip tendency as the risk for fault rupture (Yukutake et al., 2015). The probability of an earthquake occurring on certain faults is a topic that is best tackled by more appropriate neotectonic analyses. Indeed, knowledge of which faults are more likely to be reactivated in the WQSZ, and in other stable continental regions worldwide where slip tendency analysis can be applied, can help earthquake geologists narrow down which faults/areas to prioritize and focus on for more detailed active fault mapping and paleoseismic studies that can reveal earthquake magnitude and recurrence interval estimates.

Data Availability Statement

Data in this study were uploaded into the open-access Zenodo repository: western Quebec seismic zone modeled slip tendencies and slip kinematics (http://doi.org/10.5281/zenodo.4698531). Data sets for this research are also available in these in-text data citation references: Adams et al. (1988, 1989), Bent (1996), Bent et al. (2002, 2003), Du et al. (2003), Horner et al. (1978), Ma and Eaton (2007), Seeber et al. (2002), Wahlström (1987), Natural Resources Canada (NRCan; https://earthquakescanada.nrcan.gc.ca/index-en.php), and United States Geological Survey (USGS; https://www.usgs.gov/natural-hazards/earthquake-hazards/earthquakes).

Acknowledgments
Dr. Jeremy Rimando's postdoctoral fellowship at McMaster University was gratefully funded in part by the Keith MacDonald structural geology advancement fund which made this study possible. The authors would like to acknowledge Drs. Alan Vaughan and Cathal Reilly of Petroleum Experts Ltd. for their assistance with the MOVE™ Software which was kindly donated to McMaster University for academic use. The authors would also like to thank Dr. Mark Zoback (Stanford University), Dr. Elena Konstantinovskaya (University of Alberta), and Dr. Maurice Lamontagne (Geological Survey of Canada) for the very helpful discussions about the assumptions behind the parameters used for modeling slip tendency in eastern Canada. Finally, the authors thank Editor Dr. Kristy Tiampo, Dr. Dariush Motazedian, and Mr. Nicolas Harrichhausen for their constructive reviews that substantially contributed to the improvement of this manuscript.

References

Aagaard, B. T., Hall, J. F., & Heaton, T. H. (2004). Effects of fault dip and slip rake angles on near-source ground motions: Why rupture directivity was minimal in the 1999 Chi-Chi, Taiwan, earthquake. *Bulletin of the Seismological Society of America*, *94*(1), 155–170. https://doi.org/10.1785/0120030053

Adams, J. (1989). Postglacial faulting in eastern Canada: Nature, origin and seismic hazard implications. *Tectonophysics*, *163*(3–4), 323–331. https://doi.org/10.1016/0040-1951(89)90267-9

Adams, J., Sharp, J., & Stagg, M. C. (1988). *New focal mechanisms for southeastern Canadian earthquakes* (Geological Survey of Canada Open File Report 1992, p. 109). https://doi.org/10.4095/130428

Adams, J., Vonk, A., Pittman, D., & Vatcher, H. (1989). *New focal mechanisms for southeastern Canadian earthquakes* (Geological Survey of Canada Open File Report 1995, Vol. II, p. 97). https://doi.org/10.4095/130594

Atkinson, G. M., & Assatourians, K. (2010). Attenuation and source characteristics of the 23 June 2010 M 5.0 Val-des-Bois, Quebec, earthquake. *Seismological Research Letters*, *81*(5), 849–860. https://doi.org/10.1785/gssrl.81.5.849

Aylsworth, J. M., & Hunter, J. A. M. (2003). *The Ottawa Valley Landslide Project: A geophysical and geotechnical investigation of geological controls on landsliding and deformation in Leda clay* (pp. 227–234). Paper presented at the Third Canadian Conference on Geotechnique and Natural Hazards, GeoHazards.

Bent, A. L. (1995). A complex double-couple source mechanism for the Ms 7.2 1929 Grand Banks earthquake. *Bulletin of the Seismological Society of America*, *85*(4), 1003–1020.

Bent, A. L. (1996). Am improved source mechanism for the 1935 Timiskaming, Quebec earthquake from regional waveforms. *Pure and Applied Geophysics*, *146*(1), 5–20. https://doi.org/10.1007/BF00876667

Bent, A. L., Drysdale, J., & Perry, H. C. (2003). Focal mechanisms for eastern Canadian earthquakes, 1994–2000. *Seismological Research Letters*, *74*(4), 452–468. https://doi.org/10.1785/gssrl.74.4.452

Bent, A. L., Lamontagne, M., Adams, J., Woodgold, C. R., Halchuk, S., Drysdale, J., et al. (2002). The Kipawa, Quebec "Millennium" earthquake. *Seismological Research Letters*, *73*(2), 285–297. https://doi.org/10.1785/gssrl.73.2.285

Bott, M. H. P. (1959). The mechanics of oblique slip faulting. *Geological Magazine*, *96*(2), 109–117. https://doi.org/10.1017/S0016756800059987

Brooks, G. R. (2013). A massive sensitive clay landslide, Quyon Valley, southwestern Quebec, Canada, and evidence for a paleoearthquake triggering mechanism. *Quaternary Research*, *80*(3), 425–434. https://doi.org/10.1016/j.yqres.2013.07.008

Brooks, G. R. (2014). Prehistoric sensitive clay landslides and paleoseismicity in the Ottawa valley, Canada. In *Landslides in sensitive clays* (Vol. 9, pp. 119–131). Springer. https://doi.org/10.1007/978-94-007-7079-9_10

Brooks, G. R. (2015). An integrated stratigraphic approach to investigating evidence of paleoearthquakes in lake deposits of Eastern Canada. *Geoscience Canada*, *42*(2), 247. https://doi.org/10.12789/geocanj.2014.41.063

Brooks, G. R., & Adams, J. (2020). A review of evidence of glacially-induced faulting and seismic shaking in eastern Canada. *Quaternary Science Reviews*, *228*, 106070. https://doi.org/10.1016/j.quascirev.2019.106070

Busch, J. P., van der Pluijm, B. A., Hall, C. M., & Essene, E. J. (1996). Listric normal faulting during postorogenic extension revealed by 40Ar/39Ar thermochronology near the Robertson Lake shear zone, Grenville orogen, Canada. *Tectonics*, *15*(2), 387–402. https://doi.org/10.1029/95TC03501

Byerlee, J. (1978). Friction of rocks. *Pure and Applied Geophysics*, *116*, 615–626. https://doi.org/10.1007/BF00876528

Calais, E., Camelbeeck, T., Stein, S., Liu, M., & Craig, T. J. (2016). A new paradigm for large earthquakes in stable continental plate interiors. *Geophysical Research Letters*, *43*(20), 10621–10637. https://doi.org/10.1002/2016GL070815

Collettini, C., & Trippetta, F. (2007). A slip tendency analysis to test mechanical and structural control on aftershock rupture planes. *Earth and Planetary Science Letters*, *255*(3–4), 402–413. https://doi.org/10.1016/j.epsl.2007.01.001

Culotta, R. C., Pratt, T., & Oliver, J. (1990). A tale of two sutures: COCORP's deep seismic surveys of the Grenville province in the eastern US midcontinent. *Geology*, *18*(7), 646–649. https://doi.org/10.1130/0091-7613(1990)018<0646:atotsc>2.3.co;2

Daneshfar, B., & Benn, K. (2002). Spatial relationships between natural seismicity and faults, southeastern Ontario and north-central New York state. *Tectonophysics*, *353*(1–4), 31–44. https://doi.org/10.1016/S0040-1951(02)00279-2+C12:X13

den Hartog, S. A. M., Faulkner, D. R., & Spiers, C. J. (2020). Low friction coefficient of phyllosilicate fault gouges and the effect of humidity: Insights from a new microphysical model. *Journal of Geophysical Research: Solid Earth*, *125*(6), e2019JB018683. https://doi.org/10.1029/2019JB018683

DePolo, C. M. (1989). *Historical Basin and Range Province surface faulting and fault segmentation segmentation. Fault Segmentation and Controls of Rupture Initiation and Termination* (U.S. Geological Survey Open File Report No. 89–315, pp. 131–162).

DePolo, C. M., Clark, D. G., Slemmons, D. B., & Ramelli, A. R. (1991). Historical surface faulting in the Basin and Range province, western North America: Implications for fault segmentation. *Journal of Structural Geology*, *13*(2), 123–136. https://doi.org/10.1016/0191-8141(91)90061-M

Dineva, S., Eaton, D., Ma, S., & Mereu, R. (2007). The October 2005 Georgian Bay, Canada, earthquake sequence: Mafic Dykes and their role in the mechanical heterogeneity of Precambrian crust. *Bulletin of the Seismological Society of America*, *97*(2), 457–473. https://doi.org/10.1785/0120060176

Doughty, M., Eyles, N., & Eyles, C. (2012). High-resolution seismic reflection profiling of neotectonic faults in Lake Timiskaming, Timiskaming Graben, Ontario-Quebec, Canada. *Sedimentology*, *60*(4), 983–1006. https://doi.org/10.1111/sed.12002

Du, W. X., Kim, W. Y., & Sykes, L. R. (2003). Earthquake source parameters and state of stress for the northeastern United States and southeastern Canada from analysis of regional seismograms. *Bulletin of the Seismological Society of America*, *93*(4), 1633–1648. https://doi.org/10.1785/0120020217

Dupin, J. M., Sassi, W., & Angelier, J. (1993). Homogeneous stress hypothesis and actual fault slip: A distinct element analysis. *Journal of Structural Geology*, *15*(8), 1033–1043. https://doi.org/10.1016/0191-8141(93)90175-A

Dyke, A. S., Andrews, J. T., Clark, P. U., England, J. H., Miller, G. H., Shaw, J., & Veillette, J. J. (2002). The Laurentide and Innuitian ice sheets during the last glacial maximum. *Quaternary Science Reviews*, *21*(1–3), 9–31. https://doi.org/10.1016/S0277-3791(01)00095-6

George, N. V., Tiampo, K. F., Sahu, S. S., Mazzotti, S., Mansinha, L., & Panda, G. (2012). Identification of glacial isostatic adjustment in Eastern Canada using S transform filtering of GPS observations. *Pure and Applied Geophysics*, *169*(8), 1507–1517. https://doi.org/10.1007/s00024-011-0404-1

Goda, K. (2019). Nationwide earthquake risk model for wood-frame houses in Canada. *Frontiers in Built Environment*, *5*, 128. https://doi.org/10.3389/fbuil.2019.00128

Hasegawa, H. S., Adams, J., & Yamazaki, K. (1985). Upper crustal stresses and vertical stress migration in eastern Canada. *Journal of Geophysical Research*, *90*(B5), 3637–3648. https://doi.org/10.1029/JB090iB05p03637

Hasegawa, H. S., & Kanamori, H. (1987). Source mechanism of the magnitude 7.2 Grand Banks earthquake of November 1929: Double couple or submarine landslide? *Bulletin of the Seismological Society of America*, *77*(6), 1984–2004.

Heidbach, O., Tingay, M., Barth, A., Reinecker, J., Kurfeß, D., & Müller, B. (2010). Global crustal stress pattern based on the World Stress Map database release 2008. *Tectonophysics*, *482*(1–4), 3–15. https://doi.org/10.1016/j.tecto.2009.07.023

Horner, R. B., Stevens, A. E., Hasegawa, H. S., & Leblanc, G. (1978). Focal parameters of the July 12, 1975, Maniwaki, Québec, earthquake—An example of intraplate seismicity in eastern Canada. *Bulletin of the Seismological Society of America*, *68*(3), 619–640.

Ito, T., & Zoback, M. D. (2000). Fracture permeability and in situ stress to 7 km depth in the KTB scientific drillhole. *Geophysical Research Letters*, *27*(7), 1045–1048. https://doi.org/10.1029/1999GL011068

Kay, G. M. (1942). Ottawa-Bonnechere graben and Lake Ontario homocline. *Bulletin of the Geological Society of America*, *53*(4), 585–646. https://doi.org/10.1130/GSAB-53-585

Knuepfer, P. L. K. (1989). *Implications of the characteristics of end-points of historical surface fault ruptures for the nature of fault segmentation. Fault Segmentation and Controls of Rupture Initiation and Termination* (U.S. Geological Survey Open File Report No. 89–315, 193–228).

Kovacs, P. (2010). *Reducing the risk of earthquake damage in Canada: Lessons from Haiti and Chile*. Institute for Catastrophic Loss Reduction. Retrieved from https://www.iclr.org/wp-content/uploads/PDFS/lessons-from-haiti-and-chile.pdf

Kumarapeli, P. S. (1978). The St. Lawrence paleo-rift system: A comparative study. In *Tectonics and geophysics of continental rifts* (pp. 367–384). Springer. https://doi.org/10.1007/978-94-009-9806-3_29

Lamontagne, M., Brouillette, P., Grégoire, S., Bédard, M. P., & Bleeker, W. (2020). *Faults and lineaments of the western Quebec seismic zone, Quebec and Ontario* (Open File 8361, p. 28). Geological Survey of Canada. https://doi.org/10.4095/321900

Lamontagne, M., & Ranalli, G. (1996). Thermal and rheological constraints on the earthquake depth distribution in the Charlevoix, Canada, intraplate seismic zone. *Tectonophysics*, *257*(1), 55–69. https://doi.org/10.1016/0040-1951(95)00120-4

Le Pan, N. (2016). *Fault lines: Earthquakes, insurance, and systemic financial risk* (Vol. 454). CD Howe Institute Commentary. Retrieved from https://www.cdhowe.org/sites/default/files/attachments/research_papers/mixed/Commentary%20454_0.pdf

Lisle, R. J. (2013). A critical look at the Wallace-Bott hypothesis in fault-slip analysis. *Bulletin de la Societe Geologique de France*, *184*(4–5), 299–306. https://doi.org/10.2113/gssgfbull.184.4-5.299

Lisle, R. J., & Srivastava, D. C. (2004). Test of the frictional reactivation theory for faults and validity of fault-slip analysis. *Geology*, *32*(7), 569–572. https://doi.org/10.1130/G20408.1

Lovell, H. L., & Caine, T. W. (1970). *Lake temiskaming Rift Valley* (Ontario Department of Mines Miscellaneous Paper 39, p. 16). Retrieved from http://www.geologyontario.mndm.gov.on.ca/mndmfiles/pub/data/records/MP039.html

Ma, S., & Audet, P. (2014). The 5.2 magnitude earthquake near Ladysmith, Quebec, 17 May 2013: Implications for the seismotectonics of the Ottawa–Bonnechere Graben. *Canadian Journal of Earth Sciences*, *51*(5), 439–451. https://doi.org/10.1139/cjes-2013-0215

Ma, S., & Eaton, D. W. (2007). Western Quebec seismic zone (Canada): Clustered, midcrustal seismicity along a Mesozoic hot spot track. *Journal of Geophysical Research*, *112*(B6). https://doi.org/10.1029/2006JB004827

Ma, S., & Motazedian, D. (2012). Studies on the June 23, 2010 north Ottawa M_W 5.2 earthquake and vicinity seismicity. *Journal of Seismology*, *16*(3), 513–534. https://doi.org/10.1007/s10950-012-9294-7

Mazzotti, S., & Townend, J. (2010). State of stress in central and eastern North American seismic zones. *Lithosphere*, *2*(2), 76–83. https://doi.org/10.1130/L65.1

McCalpin, J. P. (Ed.). (2009). *Paleoseismology* (2nd ed., p. 613, International Geophysics Series). Academic Press.

Mirza, S., & Ali, M. S. (2017). Infrastructure crisis—A proposed national infrastructure policy for Canada. *Canadian Journal of Civil Engineering*, *44*(7), 539–548. https://doi.org/10.1139/cjce-2016-0468

Morell, K. D., Styron, R., Stirling, M., Griffin, J., Archuleta, R., & Onur, T. (2020). Seismic hazard analyses from geologic and geomorphic data: Current and future challenges. *Tectonics*, *39*(10), e2018TC005365. https://doi.org/10.1029/2018TC005365

Morris, A., Ferrill, D. A., & Henderson, D. B. (1996). Slip-tendency analysis and fault reactivation. *Geology*, *24*(3), 275–278. https://doi.org/10.1130/0091-7613(1996)024<0275:STAAFR>2.3.CO;2

Muir-Wood, R. (1989). Extraordinary deglaciation reverse faulting in Northern Fennoscandia. In *Earthquakes at North-Atlantic passive margins: Neotectonics and postglacial rebound* (NATO ASI Series (Series C: Mathematical and Physical Sciences), Vol. 266, pp. 141–173). Springer. https://doi.org/10.1007/978-94-009-2311-9_10

Peace, A. L., Dempsey, E. D., Schiffer, C., Welford, J. K., McCaffrey, K. J., Imber, J., & Phethean, J. J. (2018). Evidence for basement reactivation during the opening of the Labrador Sea from the Makkovik Province, Labrador, Canada: Insights from field data and numerical models. *Geosciences*, *8*(8), 308. https://doi.org/10.3390/geosciences8080308

Pollard, D. D., Saltzer, S. D., & Rubin, A. M. (1993). Stress inversion methods: Are they based on faulty assumptions? *Journal of Structural Geology*, *15*(8), 1045–1054. https://doi.org/10.1016/0191-8141(93)90176-B

Reiter, K., Heidbach, O., Schmitt, D., Haug, K., Ziegler, M., & Moeck, I. (2014). A revised crustal stress orientation database for Canada. *Tectonophysics*, *636*, 111–124. https://doi.org/10.1016/j.tecto.2014.08.006

Richardson, R. M. (1992). Ridge forces, absolute plate motions, and the intraplate stress field. *Journal of Geophysical Research*, *97*(B8), 11739–11748. https://doi.org/10.1029/91JB00475

Rimando, J., Schoenbohm, L. M., Ortiz, G., Alvarado, P., Venerdini, A., Owen, L. A., et al. (2021). Late Quaternary intraplate deformation defined by the Las Chacras Fault Zone, West-Central Argentina. *Tectonics*, *40*, e2020TC006509. https://doi.org/10.1029/2020TC006509

Rimando, R. E. (1994). *Tectonic framework and relative ages of structures within the Ottawa–Bonnechère Graben* (MSc thesis). University of Ottawa.

Rimando, R. E., & Benn, K. (2005). Evolution of faulting and paleo-stress field within the Ottawa graben, Canada. *Journal of Geodynamics*, *39*(4), 337–360. https://doi.org/10.1016/j.jog.2005.01.003

Rimando, R. E., & Knuepfer, P. L. (2006). Neotectonics of the Marikina Valley fault system (MVFS) and tectonic framework of structures in northern and central Luzon, Philippines. *Tectonophysics*, *415*(1–4), 17–38. https://doi.org/10.1016/j.tecto.2005.11.009

Rocher, M., & Tremblay, A. (2001). L'effondrement de la plate-forme du Saint-Laurent: Ouverture de Iapetus ou de l'Atlantique? Apport dela reconstitution des paléocontraintes dans la régionde Québec (Canada). *Comptes Rendus de l'Académie des Sciences Paris, Sciences de la Terre et des planets*, *333*, 171–178. https://doi.org/10.1016/S1251-8050(01)01610-X

Seeber, L., Kim, W. Y., Armbruster, J. G., Du, W. X., Lerner-Lam, A., & Friberg, P. (2002). The 20 April 2002 M_w 5.0 earthquake near Au Sable Forks, Adirondacks, New York: A first glance at a new sequence. *Seismological Research Letters*, *73*(4), 480–489. https://doi.org/10.1785/gssrl.73.4.480

Sibson, R. H. (1989). High-angle reverse faulting in northern New Brunswick, Canada, and its implications for fluid pressure levels. *Journal of Structural Geology*, *11*(7), 873–877. https://doi.org/10.1016/0191-8141(89)90104-1

Snee, J. E. L., & Zoback, M. D. (2020). Multiscale variations of the crustal stress field throughout North America. *Nature Communications*, *11*(1), 1–9. https://doi.org/10.1038/s41467-020-15841-5

Statistics Canada. (2020a). *Table 36-10-0468-01: Gross domestic product (GDP) at basic prices, by census metropolitan area (CMA) (x 1,000,000) [Data table]*. https://doi.org/10.25318/3610046801-eng

Statistics Canada (2020b). *Table 17-10-0135-01: Population estimates, July 1, by census metropolitan area and census agglomeration, 2016[Data table]*. https://doi.org/10.25318/1710013501-eng

Stein, S. (2007). Approaches to continental intraplate earthquake issues. In *Continental intraplate earthquakes: Science, hazard, and policy issue* (Vol. 425, pp. 1–16). Geological Society of American Spectrum Paper. https://doi.org/10.1130/2007.2425(0110.1130/2007.2425(01)

Stein, S., & Liu, M. (2009). Long aftershock sequences within continents and implications for earthquake hazard assessment. *Nature*, *462*(7269), 87–89. https://doi.org/10.1038/nature08502

Townend, J., & Zoback, M. D. (2000). How faulting keeps the crust strong. *Geology*, *28*(5), 399–402. https://doi.org/10.1130/0091-7613(2000)028<0399:hfktcs>2.3.co;2

Tuttle, M. P., Schweig, E. S., Sims, J. D., Lafferty, R. H., Wolf, L. W., & Haynes, M. L. (2002). The earthquake potential of the New Madrid seismic zone. *Bulletin of the Seismological Society of America*, *92*(6), 2080–2089. https://doi.org/10.1785/0120010227

Wahlström, R. (1987). Focal mechanisms of earthquakes in southern Quebec, southeastern Ontario, and northeastern New York with implications for regional seismotectonics and stress field characteristics. *Bulletin of the Seismological Society of America*, *77*(3), 891–924.

Wallace, R. E. (1951). Geometry of shearing stress and relation to faulting. *The Journal of Geology*, *59*(2), 118–130. https://doi.org/10.1086/625831

Wallach, J., Benn, K., & Rimando, R. (1995). Recent, tectonically induced, surficial stress-relief structures in the Ottawa–Hull area, Canada. *Canadian Journal of Earth Sciences*, *32*(3), 325–333. https://doi.org/10.1139/e95-027

Wallach, J., & Chagnon, J. Y. (1990). The occurrence of pop-ups in the Québec City area. *Canadian Journal of Earth Sciences*, *27*(5), 698–701. https://doi.org/10.1139/e90-068

Wallach, J. L., Mohajer, A. A., McFaII, G. H., Bowlby, J. R., Pearce, M., & McKay, D. A. (1993). Pop-ups as geological indicators of earthquake-prone areas in intraplate eastern North America. In L. A. Owen, I. Stewart, & C. Vita-Finzi (Eds.), *Neotectonics: Recent advances* (Quaternary Proceedings, Vol. 3, pp. 67–83).

Wells, D. L., & Coppersmith, K. J. (1994). New empirical relationships among magnitude, rupture length, rupture width, rupture area, and surface displacement. *Bulletin of the Seismological Society of America*, *84*(4), 974–1002.

Worum, G., van Wees, J. D., Bada, G., van Balen, R. T., Cloetingh, S., & Pagnier, H. (2004). Slip tendency analysis as a tool to constrain fault reactivation: A numerical approach applied to three-dimensional fault models in the Roer Valley rift system (southeast Netherlands). *Journal of Geophysical Research*, *109*(B2). https://doi.org/10.1029/2003JB002586

Wu, P., & Hasegawa, H. S. (1996). Induced stresses and fault potential in eastern Canada due to a realistic load: A preliminary analysis. *Geophysical Journal International*, *127*(1), 215–229. https://doi.org/10.1111/j.1365-246X.1996.tb01546.x

Xu, H., Xu, S., Nieto-Samaniego, Á. F., & Alaniz-Álvarez, S. A. (2017). Slicken 1.0: Program for calculating the orientation of shear on reactivated faults. *Computers & Geosciences*, *104*, 158–165. https://doi.org/10.1016/j.cageo.2016.07.015

Yan, J., Chen, X., Meng, G., Lü, Q., Deng, Z., Qi, G., & Tang, H. (2019). Concealed faults and intrusions identification based on multiscale edge detection and 3D inversion of gravity and magnetic data: A case study in Qiongheba area, Xinjiang, Northwest China. *Interpretation*, *7*(2), T331–T345. https://doi.org/10.1190/INT-2018-0066.1

Yukutake, Y., Takeda, T., & Yoshida, A. (2015). The applicability of frictional reactivation theory to active faults in Japan based on slip tendency analysis. *Earth and Planetary Science Letters*, *411*, 188–198. https://doi.org/10.1016/j.epsl.2014.12.005

Zoback, M. D., & Zoback, M. L. (2002). State of stress in the Earth's lithosphere. In W. H. K. Lee, P. C. Jennings, & H. Kanamori (Eds.), *International handbook of earthquake and engineering seismology* (International Geophysics Series, pp. 559–XII). Academic Press. https://doi.org/10.1016/s0074-6142(02)80237-6

Zoback, M. L. (1992). Stress field constraints on intraplate seismicity in eastern North America. *Journal of Geophysical Research*, *97*(B8), 11761–11782. https://doi.org/10.1029/92JB00221